Inertial Control Applied to Synchronverters to Achieve Linear Swing Dynamics

Deepak Deepak, David Raisz, Aysar Musa, Ferdinanda Ponci, Antonello Monti
Institute of Automation of Complex Power Systems, E.ON Energy Research Centre
RWTH Aachen University
Aachen, Germany
{ddeepak, draisz, amusa, fponci, amonti}@eonerc.rwth-aachen.de

***Abstract*—Power system stability has become a critical aspect with increasing integration of converter-interfaced generators (CIGs). The power system is evolving from synchronous generators, with high inertia and slow nature, to CIGs, with little or no-inertia and very fast dynamics. The challenge lies in the smooth transition from reliable operation with synchronous machines to operating dynamic power-electronics based generators (up to 100%). The idea is to explore the flexibility offered by Power Electronics (PE) to develop control strategies such that a linear and uniform system dynamics (LSD) can be achieved. In this paper, inertia-control is proposed to achieve LSD. This linearizes the behavior of converters and hence enables stability analysis using simple tools for linear system. Following which, a novel control law based on delta-based linearized swing equation is proposed to achieve LSD. It transforms the control problem from regulation of power to regulation of power-angle. A new constant, namely rocof constant, is defined. The dynamics equations are presented with the stability analysis. Time-domain simulation results, using MATLAB, are presented for these control strategies for a Single Machine Infinite Bus (SMIB).**

Keywords—converter-based power system dynamics, power system control, power system stability, inertial control, synchronverter, renewable sources of energy

I. INTRODUCTION

Today's power system is undergoing major changes due to environmental and sustainability concerns. This has resulted in transition of the power system from the classical Synchronous Generators (SGs) towards a converter-based power system in order to integrate Renewable energy sources (RES). The operation of the power system with the SG is well understood but the regulation and interaction of the Converter-interfaced generator (CIG) with the rest of the network is not yet fully known [1]. The difference are due to the characteristics of a CIG and a SG. The high inertia, damping-effect and self-synchronization property of a SG is responsible for operating huge inter-connected power systems with system security. The CIG with no rotating part, fast dynamics gives a different possibility to operate a fully or partial converter-based power system. This transition poses a lot of challenges and requires a *new scientific basis* to be developed for a converter-based power system. Out of the various challenges, this paper focuses on challenges in frequency stability because of low inertia power systems.

A PE-based CIG lacks physical inertia which makes a converter-based power system a low-inertia system. Consequently, new challenges regarding the system stability need to be addressed [2], [3]. One of the most advocated solution for smooth transition into the future inverter-based power system is to develop control strategies to provide synthetic inertia (SI) or virtual inertia and hence, design converters to mimic the behavior of a SG in terms of inertial response and its control behavior. The first converter mimicking the behavior of SG is proposed as Virtual Synchronous Machine (VSM) [4]. It is labeled as VISMA. Since then various other inertia emulation schemes have been proposed. These schemes can be classified on the basis of their implementation as Synchronous generator model-based, Swing equation-based, and Frequency-power response-based [5].

Other control approaches include matching control [6]. This approach tries to match the electro-mechanical energy exchange of a SG with energy exchange at the inverter between the grid-side and the DC-link. Another area of interest is virtual oscillator control. This control strategy controls the inverter to behave like a non-linear oscillator [7]. These techniques, with advantages and disadvantages, try to provide solution for the smooth transition.

For power system engineers, the challenge is to address the stability of the network when there is a vast amount of CIGs, (among them high voltage direct current transmission systems, HVDCs, [9]) with different control structures, from different manufactures and different dynamic behavior. The flexibility provided by the PE can be utilized to address these challenges. One of the approaches which addresses this concern is [8]. The motivation is to develop linear and uniform system dynamics such that the dynamics of a CIG is predictable and controllable. This could also help in addressing the multi-machine stability analysis with a simpler approach.

This paper is organized as follows. The second section explains the concept of inertial control to achieve LSD. The dynamic equations with stability analysis are presented in this section. Following, the next section introduces the novel control strategy based on the *delta-based linear swing equation* (DLSE). The system overview is presented along with operation and implementation of the controller called as *delta-based linearized swing controller* (DLSC). The dynamic equations are presented along with the stability analysis. A generalized *stability criterion* is developed for its operation. The next section explains the voltage-based LSD-SV in brief. The implementation in a SV is presented. In the simulation results section, first all the simulation parameters are presented, and then time-domain responses are presented with voltage-based LSD, inertial based LSD and delta-based LSD for power injection into the grid.

This work has been funded by the European Commission through the Horizon 2020 research and innovation programme, under the RESERVE project grant agreement No. 727481.

The authors gratefully acknowledge funding by the German Federal Ministry of Education and Research (BMBF) within the Kopernikus Project ENSURE 'New ENergy grid StructURes for the German Energiewende'.

978-1-7281-2650-0/19/$31.00 ©2019 IEEE

II. Inertial Control

A. System Dynamics

Swing equation is the fundamental equation governing rotor dynamics for a synchronous generator and is given by (1) [10].

$$J\frac{d\omega_m}{dt} = T_m - T_e - D_p(\omega - \omega_{ref}) \tag{1}$$

where J is the combined moment of inertia, ω_m is angular velocity, θ_m is angular displacement of rotor, $T_m$is mechanical torque, T_e is electrical torque, D_p is damping coefficient, and ω_{ref} is nominal or reference velocity. Equation (1) can be written in terms of electrical angle, δ and is given by (2).

$$M\frac{d^2\delta}{dt^2} = P_m - P_e - D(\omega - \omega_{ref}) \tag{2}$$

Here P_e is the power exchange between the generator and the grid and is given by (3).

$$P_e = \frac{V_c V_g}{X_g} sin\delta \tag{3}$$

where V_c is generator output voltage and V_g is grid voltage with $X_g \gg R_g$ grid reactance, δ is phase-angle between V_c and V_g. The non-linearity is present in (3) between P_e and δ with δ being the state variable. This makes the behavior of SG non-linear.

B. Inertial Control

The CIGs using PE give us additional degrees of freedom to choose M and D to achieve desired control response from the converter. The swing equation, in different forms of implementation, is the heart of different inertia-emulation schemes [9]. The desired dynamic equation for inertial-control based LSD is given by (4). The derivation of this form of equation is given in Appendix.

$$\frac{d^2\delta}{dt^2} = K^2\delta_{ref} - K^2\delta - 2K(\omega - \omega_{ref}) \tag{4}$$

where, K is the desired eigenvalue, δ_{ref} is reference power-angle, δ_e is actual power-angle. The swing equation is given in (2). By comparing (2) and (4), the expression for adaptive inertial constant, M_i can be calculated. The expression for M_i is given by (5).

$$M_i = \frac{P_m - P_e - D(\omega - \omega_{ref})}{K^2\delta_{ref} - K^2\delta - 2K(\omega - \omega_{ref})} \tag{5}$$

Similarly, the expression for adaptive inertial constant, J_i is given by (6).

$$J_i = \frac{T_m - T_e - D_p(\omega - \omega_{ref})}{K^2\delta_{ref} - K^2\delta_e - 2K(\omega - \omega_{ref})} \tag{6}$$

By using the adaptive inertial constant, M_i and J_i given by (5) and (6), respectively, linearizes the system dynamics. The dynamic equation for the system becomes as given by (4) which is linear with respect to power-angle, δ.

C. Calculation of M_i and J_i

The expression for adaptive inertia constant contains δ_e and δ_{ref}. The angle δ_e is calculated using (3) and is given by (7)

$$\delta = \sin^{-1}\left(\frac{P_e X_g}{V_c V_g}\right) \tag{7}$$

By replacing the P_e with P_m the δ_{ref} is calculated using (8)

$$\delta_{ref} = \sin^{-1}\left(\frac{P_m X_g}{V_c V_g}\right) \tag{8}$$

The V_g and X_g are estimated values of grid voltage and grid impedance, respectively.

D. Stability Analysis

Using the expression of M_i and J_i and substituting it in swing equation given by (2) and (1), the updated state-space equations become as given by (4). The state-space representation is given by (9)

$$\begin{bmatrix}\dot{\delta}\\ \dot{\omega}\end{bmatrix} = \begin{bmatrix}0 & 1\\ -K^2 & -2K\end{bmatrix}\begin{bmatrix}\delta\\ \omega\end{bmatrix} \tag{9}$$

The eigenvalues can be calculated from (9) to be

$$\lambda_{1,2} = -K, -K \tag{10}$$

where, K is a positive number. K can be chosen to achieve the desired response of converter. This is the advantage offered by the PE-based generators.

E. Implementation of Inertial Control

The expression for M_i and J_i are of the form 0/0 in steady state. This results in a numerical error for the controller. Hence, the adaptive inertia control is enabled using the tolerance in the error of the power which is given here as

$$\Delta = \left|P_m - P_e - D(\omega - \omega_{ref})\right| \tag{11}$$

Based on the value of Δ selected, the inertia control is enabled. Also, the value of M_i and J_i are passed through a low-pass filter in order to prevent oscillations when converter is returning to the equilibrium point as also mentioned in [11]. In this paper, the inertial control is implemented in a Synchronverter (SV) [10] with the voltage loop decoupled from the power-frequency control loop and no reactive power control. This is further explained in section for voltage-based LSD-SV.

III. Delta Based Linearized Swing Controller

Any power converter can be defined as static power-electronics device that regulates power by controlling the voltage magnitude and angle at its output. The power-angle is used to control active power keeping the voltage magnitude constant. The regulation of power by controlling power-angle makes the control non-linear because there exists a non-linear relation between the power-angle, δ and P_e, as can be seen in (3). The idea is to regulate power-angle directly. This control law makes this control problem a linear control problem.

A. Control Law

The swing equation in terms of power is given by (2). The power is replaced with power-angle, δ in (2) and the new equation is given here.

$$\frac{d^2\delta}{dt^2} = R_{cf}\left(\delta_{ref} - \delta - D_\delta(\omega - \omega_{ref})\right) \qquad (12)$$

This equation is named as *Delta-based Linear Swing Equation* (DLSE).

All the quantities in this equation are electrical. The constant, R_{cf} is named as *rocof constant* whose dimension is same as for ROCOF, '1/s^2'. It is the integral gain for the control law which controls the inertial response of the converter. D_δ is the angle-frequency droop constant, δ_{ref} is power-angle reference, δ is power-angle, ω is angular frequency and ω_{ref} is reference angular frequency.

B. System Configuration

The overview structure for Delta-based Swing Controller (DLSC) is given in Fig. 1. The control and the power circuit are marked in the figure. The control signals are marked in blue-color, while controller references are marked in red-color. The power circuit is shown in black color.

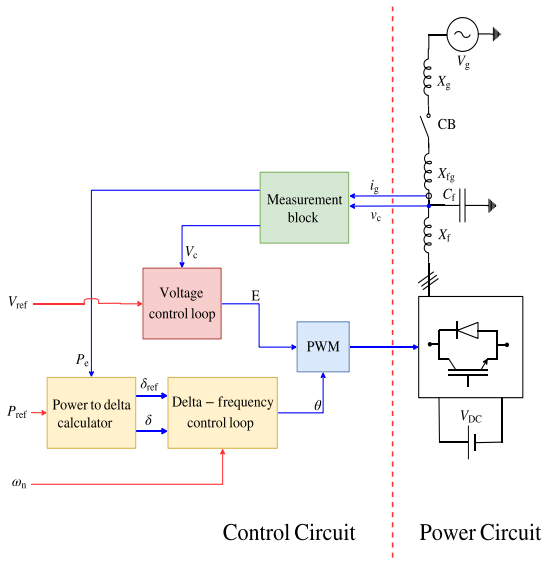

Fig. 1. System overview for DLSC.

The power-part of the converter consists of an inverter, along with the LCL-filter. The circuit breaker (CB) connects or disconnects the DLSC to the grid. The grid is a three-phase three-wire (3P3W) system. Three-phase balanced conditions are assumed for the power-circuit.

The control circuit is in the left-side of the Fig. 1. The voltage and current measurements are fed into the controller, where the DLSC is implemented. The measurement block receives the measurement from the current and the voltage sensors. The calculated power is fed into the power to delta-calculator, in which (7) and (8) are implemented. The voltage amplitude, V is fed into the voltage control loop. The input to delta-frequency loop is δ_{ref} and δ. The output of delta-frequency loop is ω which is integrated to give θ. The droop in the delta-frequency loop is implemented in the similar way as for the power-frequency droop in the synchronverter [10]. The difference in converter frequency and reference frequency is multiplied with D_δ to provide droop-angle, δ_δ which is fed back into the input as shown in Fig. 2. In the voltage control loop, the voltage amplitude is calculated from the measured capacitor voltage, V_{c}. The calculated amplitude of V_{c} is compared with reference voltage and is fed to the I-controller as shown in Fig. 2. The output of the voltage control loop is amplitude of back-emf, E.

The θ is converted into three sinusoidal functions (13) and is multiplied with E to generate three- phase reference modulation signals. This is then fed into the modulation block to generate gate-pulses for the power converter.

$$\delta \Longrightarrow [sin\theta, sin(\theta - 2\pi/3), sin(\theta + 2\pi/3)] \qquad (13)$$

The power-angles, δ and δ_{ref}, are calculated from P_{ref} and P_{e}, respectively. The control structure with the calculation of power-angles can be seen Fig. 2.

C. Operation

In the normal operation of the DLSC, the P_{ref} is increased to inject the power into the grid. From the P_{ref}, δ_{ref} is calculated using (8) and is the input for the controller. The output power, P_e, is measured and δ is calculated using (7). The error due to δ and δ_{ref} is fed into the integrator with the gain, R_{cf} and the frequency is modulated to inject the power into the grid. The voltage reference is kept constant. There is no reactive power control in DLSC.

During the disturbance in the grid-frequency, the converter increases or decreases its output power as per the frequency droop. The frequency-droop is angle-based. It means that for a change in the frequency, the converter changes δ and power corresponding to droop angle, δ_δ, is exchanged with the grid. The output power in case of grid-frequency disturbance becomes

$$P_e = P_{max}\, sin(\delta + \delta_\delta) \qquad (14)$$

where, $P_{max} = V_c * V_g / X_g$, and δ_δ is the droop-angle and is given by (15).

$$\delta_\delta = D_\delta(\omega - \omega_{ref}) \qquad (15)$$

The droop-power is dependent on the operating point as given by (14). This means that the droop-power reduces as the power-angle for the converter increases.

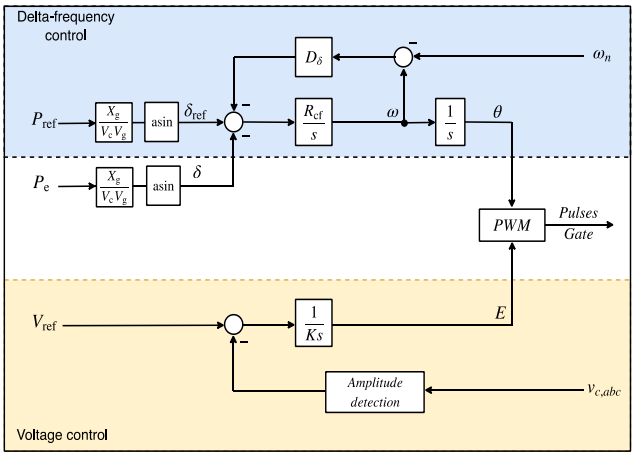

Fig. 2. Control diagram for DLSC.

The voltage loop is a simple *I*-controller with the fixed voltage reference. The voltage loop is designed faster than the delta-frequency loop and hence, its dynamics are de-coupled from delta-frequency loop.

D. Stability Analysis

The dynamic equations controlling the behavior of the DLSC are

$$\frac{d\delta}{dt} = (\omega - \omega_{ref}) \tag{16}$$

$$\frac{d\omega}{dt} = R_{cf}\left(\delta_{ref} - \delta - D_{\delta}(\omega - \omega_{ref})\right) \tag{17}$$

$$\frac{dV}{dt} = \frac{\omega_{ref}}{K}(V_{ref} - V_c) \tag{18}$$

The voltage loop is decoupled from the power-angle control and is designed faster than the delta-based linearized swing equation. Hence, for stability analysis only the critical or slow eigenvalues from DLSE are considered.

The state-space representation for DLSC is given by

$$\begin{bmatrix}\dot{\delta}\\ \dot{\omega}\end{bmatrix} = \begin{bmatrix}0 & 1\\ -R_{cf} & -R_{cf} * D_{\delta}\end{bmatrix}\begin{bmatrix}\delta\\ \omega\end{bmatrix} \tag{19}$$

The eigenvalues from (19) can be calculated to be

$$\lambda_{1,2} = \frac{-R_{cf} * D_{\delta} \pm \sqrt{(R_{cf} * D_{\delta})^2 - 4R_{cf}}}{2} \tag{20}$$

If for an inverter, $\gamma = (R_{cf} * D_{\delta})/2$, then the eigenvalues are given by

$$\lambda_{1,2} = -\gamma \pm \sqrt{\gamma^2 - R_{cf}} \tag{21}$$

For controller parameters, R_{cf} and D_{δ} can be chosen to control the response of the inverter. For oscillation free response of converter following condition is to be fulfilled:

$$\gamma^2 > R_{cf} \tag{22}$$

IV. Voltage Based LSD-Synchronverter

The voltage-based approach to achieve LSD is explained in [8]. In this paper, the voltage-based approach is implemented in a synchronverter (SV) naming it as voltage-based LSD-SV.

The control law for the voltage loop is given by (23)

$$P_e \Rightarrow \delta(P_e) = \frac{P_e X_g}{(1-\varepsilon)V^2} \Rightarrow V_{ref}(\delta) = \frac{(1-\varepsilon)V}{\sin\delta}\delta \tag{23}$$

The LSD is implemented in the SV by making changes in the control structure of the SV. The steps are given below:

1. The reactive power control is eliminated and hence the voltage control loop as voltage is directly controlled at the converter terminal.
2. The voltage control loop is decoupled from the power-frequency control loop by replacing ω with ω_{ref} in calculation of the back-emf voltage.
3. The dynamic equation for the voltage control loop becomes (18).
4. The voltage reference is calculated using the control law designed in [8] from P_e using (23).

The voltage-based LSD-SV control structure is given in Fig. 6. in the Appendix.

V. Simulations and Results

The test system is SMIB system as shown in Fig. 3. The system is 400 V, 50 Hz, 3P3W. The converter is connected with the grid through a LCL-filter. Parameters of the system are given in TABLE I. The inertia-control is implemented using the synchronverter technology with modification and control structure is given in Fig. 7. in the Appendix. The simulation is done for power injection into the grid by the converter. The results are presented for power injection into the grid. The results are shown for three controllers, voltage-based LSD-SV, inertia-based LSD-SV and DLSC. LSD-SV.

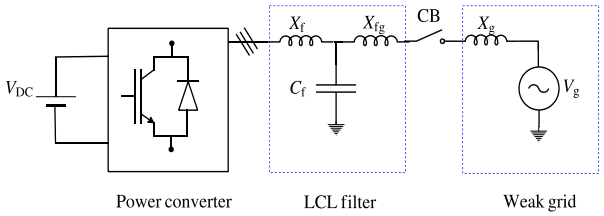

Fig. 3. Test system overview.

All the converters are connected to the grid at $t = 0.5$ s. The synchronization logic is not explained in this paper. The P_{ref} for converter is increased from $t = 1$ s. At every second, the P_{ref} is increased by 0.2 p.u. until 1.0 p.u. at $t = 5$ s.

TABLE I. Model Parameters for SMIB Simulations

Nominal Voltage	V_n	400	V
Nominal angular frequency	ω_{ref}	314.14	rad/s
Converter Power rating	S_n	80.00	KVA
DC-link Voltage	V_{DC}	750.00	V
Converter-side filter inductance	L_f	1.00	mH
Filter capacitor	C_f	10.96	μF
Grid-side filter inductance	L_{fg}	0.30	mH
Grid impedance	X_g	0.31	Ω
Moment of inertia	J	0.96	Kg/m^2
Frequency-Droop constant	D_p	38.52	W/rad/s
Voltage-Intergal gain	K	0.025	rad
Rocof constant	R_{cf}	400.00	1/s^2
Delta-Droop constant	D_{δ}	0.10	1/s
Tolerance for inertia control	Δ	0.1	Nm

A. Power Response

Fig. 4 shows the power response for all the three controllers implementing LSD characteristics. As it can be seen that rise time and settling time for each step-change in P_{ref} for all the three controllers are approximately same. The response is over-damped in all the step-changes for all the controller.

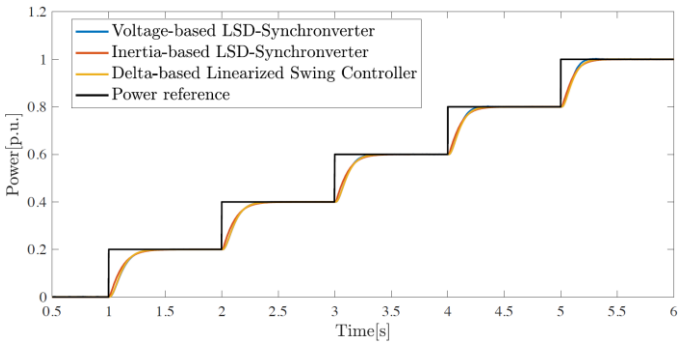

Fig. 4. Power response for LSD-based converters.

B. *Frequency Response*

The frequency response is shown in Fig. 5. The frequency response inertia-based LSD-SV and DLSC is slower at $t = 5$ s and this is because the regulation of power is replaced with regulation of angle and hence, increase in power-angle is more to achieve the same step-increase in the power due to the sinusoidal P- δ characteristics. But for the voltage-based LSD-SV, the increase in δ is the same because the P- δ curve is linearized by manipulating the voltage reference for the controller. This is the same reason for difference in the frequency response for the controllers. The response of all the three controllers is over-damped because of the real eigenvalues.

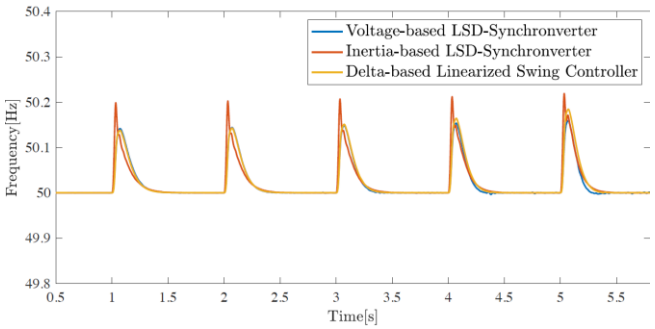

Fig. 5. Frequency response for LSD-based converters.

VI. Conclusions

The inertia control is presented with the stability analysis and the time-domain response for inertial control implemented in the SV. The inertia-based LSD-SV achieves LSD with the voltage control decoupled from power-frequency control. With the generalized expression for inertia constant M, it can be included in any of the grid inertia emulation schemes. The advantage is that LSD characteristic can be achieved independent of power-angle limit, but it is enabled using tolerance based on error in the power.

Based on the inertia-based control developed, a novel control strategy, named as delta-based linearized swing controller (DLSC) is proposed. A new constant, named as rocof constant, is also defined. A generic stability condition is derived by expressing it in terms of damping or droop constant and rocof constant with no dependency on the grid parameters. For the above implementations, the time-domain simulation results are presented for the step-increase in the power. The authors are working on implementing the control using local measurements and possible solution for implementation of LSD in multi-machine system.

References

[1] F. Milano et al., “Foundations and challenges of low-inertia systems,” (invited paper), in: 2018 Power Systems Computation Conference (PSCC). IEEE, 2018. doi: 10.23919/pscc.2018.8450880.

[2] A. Ulbig, T. S Borsche, and G. Andersson. “Impact of low rotational inertia on power system stability and operation,” in: IFAC Proceedings Volumes 47.3 (2014), pp. 7290–7297.

[3] T. S Borsche, T. Liu, and D. J. Hill. “Effects of rotational iner tia on power system damping and frequency transients,” in: 2015 54th IEEE conference on decision and control (CDC). IEEE. 2015, pp. 5940–5946.

[4] H.-P. Beck and R. Hesse, “Virtual synchronous machine,” in: 2007 9th International Conference on Electrical Power Quality and Utilisation. IEEE, 2007. doi: 10.1109/epqu.2007.4424220.

[5] U. Tamrakar et al., “Virtual inertia: Current trends and future directions,” in: Applied Sciences 7.7 (2017), p. 654.

[6] C. Arghir, T. Jouini, and F. Dörfler. “Grid-forming control for power converters based on matching of synchronous machines”. In: Automatica 95 (2018), pp. 273–282. doi: 10.1016/j.automatica.2018.05.037.

[7] S. V. Dhople, B. B. Johnson, and A. O. Hamadeh. “Virtual oscillator control for voltage source inverters,” in: 2013 51st Annual Allerton Conference on Communication, Control, and Computing (Allerton). IEEE, 2013. doi: 10.1109/allerton.2013.6736685.

[8] D. Raisz et al., “Linear and uniform system dynamics of future converter – Based power systems,” in: 2018 IEEE Power & Energy Society General Meeting (PESGM). IEEE. 2018, pp. 1–5.

[9] A. Musa, A. Kaushal, S. K. Gurumurthy, D. Raisz, F. Ponci, and A. Monti, "Development and stability analysis of LSD-based virtual synchronous generator for HVDC systems," IECON 2018 – 44th Annual Conference of the IEEE Industrial Electronics Society, Washington, DC, 2018, pp. 3535-3542.

[10] S. D’Arco and J. A. Suul, “Virtual synchronous machines—Classification of implementations and analysis of equivalence to droop controllers for micro-grids,” in: 2013 IEEE Grenoble Conference, IEEE, 2013, pp. 1–7.

[11] J. Machowski, J. Bialek, and J. Bumby, Power System Dynamics: Stability and Control. John Wiley & Sons, 2011.

Appendix

A. *Desired Linear system dynamics in case of inertial control*

The dynamic equation from the voltage-based LSD approach is given by [8]

$$M\frac{d\omega}{dt} = P_m - P_e - D\left(\omega - \omega_{ref}\right) \tag{A1}$$

The eigenvalues are given by

$$-\frac{D}{2M} \pm \sqrt{\frac{D^2}{4M^2} - \frac{(1-\varepsilon)\,V_g^2}{M\,X}} \tag{A2}$$

To place the eigenvalues at -K and -K, the expression for D and M becomes

$$M = \frac{(1\ -\ \varepsilon)\,V_g^2}{K^2\,X} \tag{A3}$$

$$D = \frac{2\,(1\ -\ \varepsilon)\,V_g^2}{K\ X} \tag{A4}$$

Using the expression for D and M from (A3) and (A4), (A1) becomes

$$\frac{d\omega}{dt} = K^2\delta_{ref} - K^2\delta - 2K\left(\omega - \omega_{ref}\right) \tag{A5}$$

B. *Control Diagram of Voltage- and Inertia-Based LSD-SV*

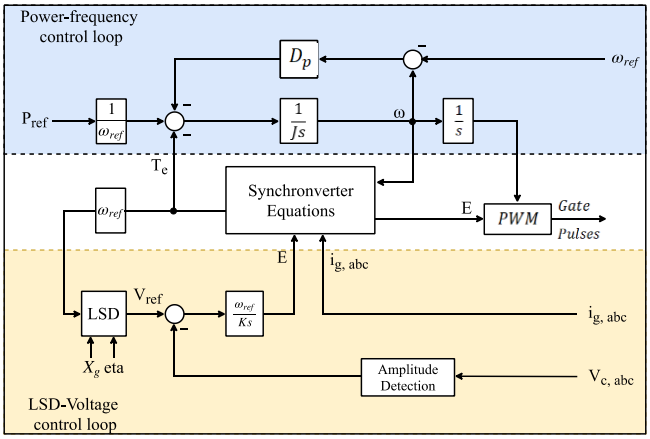

Fig. 6. Control diagram for voltage-based LSD-SV.

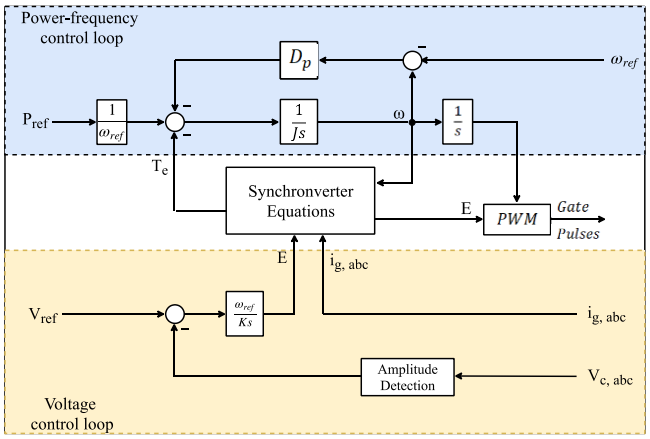

Fig. 7. Control diagram for inertia-based LSD-SV.

BIOGRAPHIES

Deepak Deepak was born in Agra, India in 1989. He graduated from U.V.C.E., Bangalore, India in 2012. He has worked in Reliance Industries Ltd, India from 2012 to 2016 as a commissioning engineer. In 2016, he started his masters in M.Sc. Electrical Power Engineering at RWTH Aachen University, Germany. Currently he is in the final-phase of his masters degree. His area of interests include application of power electronics in the power systems, and control and stability for the converter-based power systems and HVDC.

David Raisz (M'06-SM'18) received his M.Sc degree and his PhD in Electrical Engineering from Budapest University of Technology and Economics (BUTE), Budapest, Hungary, in 2000 and 2011 respectively. From 1999 to 2001 he joined Graz University of Technology, Austria, as a guest researcher. From 2012 until 2016 he led the Power Systems and Environment Group at the Dept. of Electric Power Engineering at BUTE, as Associate Professor. In 2017 he joined the Institute for Automation of Complex Power Systems within the E.ON Energy Research Center at RWTH Aachen University. He has been working on or leading more than 40 industrial and research projects.

Aysar Musa received the B.Sc. degree in power engineering from University of Mosul, Mosul, Iraq, in 2004, and the M.Sc degree in electrical and electronic engineering from University of Eastern Mediterranean, Famagusta, North Cyprus, in 2013. From 2005 to 2011, he was an Operating System Engineer in the Northern Transmission Electrical Networks, Ministry of Electricity, Iraq. In 2013, he became a Senior Power Systems Engineer. Since 2014, he has been a Research Associate with the Institute for Automation of Complex Power Systems, E.ON Energy Research Center, RWTH Aachen University. His research interests include renewable energy integration, as well as control and stability of low-inertia power systems and hybrid AC/DC networks.

Ferdinanda Ponci (M'00–SM'08) received thePh.D. degree in electrical engineering from thePolitecnico di Milano, Milan, Italy, in 2002. She joined the Department of Electrical Engineering, University of South Carolina, Columbia, SC,USA, as an Assistant Professor in 2003, and became an Associate Professor in 2008. In 2009, she joined the Institute for Automation of Complex Power Systems, RWTH Aachen University, Aachen, Germany, where she is currently a Professor of monitoring and distributed control for power systems. She is a Senior Member of the AdCom of the IEEE Instrumentation and Measurement Society.

Antonello Monti (SM'2002) received his M.Sc degree (summa cum laude) and his PhD in Electrical Engineering from Politecnico di Milano, Italy in 1989 and 1994 respectively. He started his career in Ansaldo Industria and moved in 1995 to Politecnico di Milano as Assistant Professor. In 2000 he joined the Department of Electrical Engineering of the University of South Carolina (USA) as Associate and then Full Professor. Since 2008 he is the director of the Institute for Automation of Complex Power System within the E.ON Energy Research Center at RWTH Aachen University. Dr. Monti is author or co-author of more than 300 peer-reviewed papers published in international Journals and in the proceedings of International conferences. He is a Senior Member of IEEE, Associate Editor of the IEEE System Journal, Associate Editor of IEEE Electrification Magazine, Member of the Editorial Board of the Elsevier Journal and Sustainable Energy, Grids and Networks, and member of the founding board of the Springler Journal Energy Informatics. Dr. Monti is the recipient of the 2017 IEEE Innovation in Societal Infrastructure Award.